Indonesian Journal of Electrical Engineering and Informatics (IJEEI)
Vol. 11, No. 1, March 2023, pp. 61~76
ISSN: 2089-3272, DOI: 10.52549/ijeei.v11i1.3573

An Improved Energy Saving Technique for Wireless Power Transfer in Near Field Communication Systems

Khadeejah A Abdulsalam[1], Kingsley C. Ijike[2], John A Adebisi[3]
[1,2]Department of Electrical Electronics and Computer Engineering, University of Lagos, Lagos
[3]Department of Electrical and Computer Engineering, University of Namibia, Namibia

Article Info

Article history:

Received Dec 16, 2021
Revised Dec 16, 2022
Accepted Feb 15, 2023

Keywords:

Energy efficiency
Communication
Near field communication
Power transfer
Wireless devices

ABSTRACT

In this work, an improved communication algorithm was developed to reduce energy wastage in a Near Field Communication (NFC) system using dynamic field Strength scaling technique. With a variable resistor in the reader coil, the field strength of the system was scaled in real-time by adjusting the value of the resistor in relation to distance. This system was tested with the advanced design system's Application Extension Language (AEL) and simulated on Advanced Digital Technology. The results showed a responsive change in the magnetic field when the two scenarios (with and without optimization) were simulated. There was a 66% change in energy transfer within the time frame referenced. Results further indicated that the adoption of the proposed algorithm could help engineers to design a more effective NFC system.

Corresponding Author:

John A Adebisi,
Department of Electrical and Computer Engineering,
University of Namibia,
Ongwediva Township, Namibia.
Email: adebisi_tunji@yahoo.com

1. INTRODUCTION

The Near Field Communication (NFC) is a Radio Frequency Identification (RFID) influenced communication protocol in which power and data transfer from the initiator (reader) to the target (tag or transponder) occurs typically within a distance of 10-cm and at a frequency of 13.56 MHz[1]. In the passive mode, the initiator carries out the dual function of supplying sufficient power to energize the target; this is achieved by inductive coupling and providing the RF field usually modulated for information exchange [2]. Based on the distance from a radiating antenna, there are three distinct spatial regions with varied characteristics used for different applications of data and power transfer [3-4]: the reactive near field, the radiative near field, and the far field. In this study, the reactive near field is very important, where the power transfer is achieved by inductive coupling. It is defined as the region $R \leq 0.62\sqrt{\frac{D^3}{\lambda}}$, given: R as the distance from the reader coil, λ is the wavelength at the specified frequency, and D is the largest dimension of the coil [5]. Operating within this region limits the amount of power that can be transferred, and the maximum distance between the reader and tag. NFC systems have become increasingly popular because of their ease of use in access control and wearable devices [6], depth of penetration in biological systems and security. In addition, COVID-19 and the emergence of non-contact transactions [7] have improved the relevance of NFC. The consistent development of monetary transactions and access control market using NFC has driven the aggressive deployment of NFC readers in gadgets, stores, and different infrastructures [8]. The design of NFC readers are structured for maximum field strength requirements [9]. There is a relationship between the quality of the magnetic field and the induced voltage in NFC systems [10].

Transmitting at the highest field quality also boosts the reading range [11], which provides the best communication experience for the user, as opposed to saving power. The drawback of this, however, is the tag

becomes oversupplied when its distance from the reader becomes very small [12]. This oversupplied voltage is excess energy that can be saved. Albeit tags are designed with an overvoltage protection circuit [13]. This is a system that will ensure that the oversupply never happens is most desirable as a means of conserving energy. In wireless communication conservation of energy is crucial, especially in remote areas or scenarios where a high level of mobility is required[14]. A typical localized example of this is the use of card readers and voter cards during elections. A well-documented experiment carried out by [15] revealed that; mobile phones with NFC capabilities consume more energy than those without it. Moreover, this power drain increases significantly from about 5 mW when in standby mode to about 40 mW when active [10]. Consequently, power optimization techniques for NFC systems are an ongoing field of research. Some techniques have been proposed and developed for optimizing the energy use of the reader-tag system, many of which are impracticable due to bulkiness, cost, or speed [16-18]. The solutions are also limited to a specific coil geometry (circular or rectangular). Some of these techniques include: designing systems that can switch between coils of different Q factors. Reducing the physical relation factors (the physical relation factors are the geometry of the coils, their axial alignment, distance apart, number of coils, and physical dimensions). An alternative is to design the *H*-field of the reader antenna to dynamically adjust to changes in the physical relation factors by determining its Power Transfer Function (PTF). Dynamic Field Strength Scaling is an optimization technique that uses the observer-controller principle to dynamically control the strength of the magnetic field between the reader and tag coils based on the observed properties[12], [19]. In this work, the algorithm to dynamically scale the magnetic field strength *H*, (a function of the physical relation factors, permeability, and circuitry component values) is greatly simplified by using Keysight's Advanced Design System (ADS) as the design tool.

NFC devices are designed for data transmission, not primarily for Wireless Power Transfer (WPT) [20]. There is a fundamental trade-off between the Q-factor and the bandwidth of communication. Increasing the Q will ensure higher power is being delivered to the load (higher power delivery to load-PDL), but the bandwidth of communication will be narrowed [20-21]. An inherent difficulty in dynamically scaling the magnetic field to conserve energy also exists. This is because of the constant alteration of the coupling coefficient is directly affected by the distance between the coils. This in turn, affects the power transfer function during runtime [23]. Existing methods attempt to solve these problems with some degree of success, but they are limited by the geometrical form of the antennas and models that do not consider impedance matching, leading to low efficiency, detailed in subsequent sections. This work seeks solution where there can be a balance between the power delivered to the load (PDL), and effective communication (transfer of information) between the sender and receiver.

2. LITERATURE REVIEW

2.1 Developments in Wireless Power Transfer (WPT)

WPT, a term commonly used in the description of electrical power signals from a sender to a receiver without the use of physical wires. WPT occurs either in the near field ($d < \lambda$) or far field ($d >> \lambda$), where d is the operating distance and λ is the wavelength at the specified frequency). Transfer in the near field is nonradiative. It is achieved by coupling because of its relatively smaller distance. This coupling is either by magnetic resonance or induction. For the far field, WPT is achieved through the transmission of RF waves by directional or non-directional antennas. There are health concerns associated with Radiative WPT; therefore, they are not readily used [23-24]. Furthermore, far-field power transfer is limited by directivity, as the emitter and receiver require a direct line of sight connection for power transfer, while near field power transfer systems are limited by range.

Shadid et al. [26] worked on WPT and presented comparisons of the different WPT methods. The authors in [27], wrote on the timeline of the application of WPT in the biomedical field and tabled literature in the subject up to 2017. The study emphasized inductive WPT, which is preferred for implants because of the risk of battery breakage or the inconvenience of repeated surgeries. Ref. [28] carried out a research application of WPT in the health care industry for Optogenetic implants in which WPT is used to power a mini-Light Emitting Diode (LED) that was implanted and can be remotely powered at 5 mm. [29], investigated the efficiency of WPT based on multi-auxiliary transmitting coils. It was discovered that WPT efficiency is increased when coils are placed between the source and receiver coils, depending on their number.

2.2. Developments in Near Field Communication

NFC is a half-duplex communication protocol developed in 2002 by Sony and Philips for easy and secure contactless communication between two compatible devices, typically within 10cm, with a 13.56 MHz operating frequency[29-30]. It has data rates of 106, 212, 424 kbps, and 828 kbps (but lack compliance with the standard ISO/IEC 18092 and, therefore, is not officially listed)[30]. NFC is reliant on the inductive coupling between transmitting and receiving devices. Initially, it was made to enhance mobile payments and ticketing

applications[32]. The NFC protocol identifies two modes of communication - Active and Passive[33]. In the passive mode, the reader generates a field while the tag modulates the existing field (load modulation). The supply of power is by the initiator, and the transponder (the target) draws its operating power from the electromagnetic field that is provided by the initiator. In the active mode - however, the reader and tag have their power supply and the communication between them is achieved on an alternate generation of their magnetic fields: one device disengages its transmission while awaiting the other[33]. For data transfer, NFC uses modulation schemes like Amplitude Shift Keying (ASK) with a different modulation depth of - 100 or 10%, or load modulation and coding techniques like Modified Miller, Non-Return-to-Zero Level (NRZ-L), and Manchester coding. In addition to the communication modes, NFC devices operate in one of the following modes**:** Peer-to-peer, Reader/Writer and Card Emulation.

NFC concept in smartphones was introduced by [34] although commouncatin concepts have been proven to be applicable in diverse areas [7], [35-37]; since then, numerous publications have been written on its integration [32], [38], [39], security [17], [40], [41] and software/application development [38], [42], [43]. Other studies; [40-41] have investigated the structures of NFC antennas, which influence their sensitivity, and hence general communication efficiency. A comprehensive survey of NFC technology was provided by [30], and [33], including a summary of the historical development and deployment of NFC.

The application of NFC technology can be further extended to sensing and computation with the inclusion of low-energy microcontrollers. [13] presented a device called NFC Wireless Identification and Sensing Platform (WISP). This can store excess power harvested through a single high-Quality factor (Q) receiver antenna and a multi-stage rectifier in a supercapacitor or thin-film battery. NFC readers can effectively wirelessly deliver ultra-low power to passive NFC tags through a coupled magnetic field by the principle of magnetic induction. In [8], a study to optimize power and communication with 2 and 3-coil receiver models was presented. It is observed that a 2-coil system performs better at close range, while a 3-coil system performs better at longer range. The NFC WISP is improved in [20], in a recent study that uses a switchable receiver antenna to zoptimize Power Delivery to Load (PDL) and the communication in NFC devices. A summary of selected works on NFC WPT optimization is presented in Table I.

Table 1. Summary Of Selected Literature On NFC WPT Optimization

S/N	Author	Contribution	Conclusion	Limitation
1.	N. Druml *et al.* [9]	Adaptive Field Strength Scaling (AFSS). Request-based (software) and Instantaneous Power Consumption based (hardware)	Reader/smart system's energy consumption is reduced by up to 54%	The software implementation is slow and decreases the system's maximum transfer rate. Does not cover changes in the distance at runtime
2.	M. Menghin *et al.* [46]	4-part model; Power Transfer Function (PTF) determinator. PTF is determined at runtime and is used to scale the magnetic field	Energy saved is up to 44.17%	Restricted to rectangular coils. Does not cover changes in the distance at runtime
3.	M. Menghin *et al.*[12]	NFC-DynFS. An improvement of the previous metod s outlined, as dynamic adaptation is introduced. Both oversupply and undersupply are prevented.	26% of energy is saved, and undersupply protection is achieved.	Restricted to rectangular coils.
4.	M. Menghin [10]	META[:SEC:]. A toolkit for developing power optimized NFC systems. Introduction of the 2-stage implementation of dynamic field strength scaling.	26% of energy is saved in the first implementation, and 34% is saved in the second implementation	More design patterns for power management are presented
5.	Y. Zhao et al.[20]	A technique that uses a programmable RF switch to alternate between a 2-coil and 3-coil configuration for the NFC system; A special tag (NFC WISP) that includes an e-ink display.	Reading distance improved from 0.5 cm to 1.5 cm, and the power delivered is two times more power than in [13]	Low reading distance, no true dynamic adaptation

2.3. Mathematical Principle

This section presents a set of equations that define the relationship between the electrical and magnetic factors that constitute the electromagnetic field. Maxwell's equations were used in the description of charged matter behaviour in several forms. The integral form is as stated in (1) – (4). Equation (1) is Ampere's law stating the intensity of the magnetic field around a closed path is equal to the free current flowing through the surface bounded by the path. This law, together with Faraday's law Equation (2) govern electromagnetic induction and WPT.

$$\oint_C H \cdot dl = \int_S \left(J + \frac{\partial D}{\partial t}\right) \cdot ds \quad (1)$$

$$\oint_C E \cdot dl = -\int_S \left(\frac{\partial B}{\partial t}\right) \cdot ds \quad (2)$$

$$\oint_S B \cdot ds = 0 \quad (3)$$

$$\oint_S D \cdot ds = \int_V \rho dv \quad (4)$$

From (11) every flowing current is associated with a magnetic field. The relationship is further illustrated in Equation (5)

$$\sum I = \oint \vec{H} \cdot \vec{d}\, s \quad (5)$$

The magnetic field strength around a conductor loop (round coil) is not constant but reduces at the distance from the centre of the coil increases. Equation (6) is used to determine the path of the magnetic field strength along the x-axis, according to [47].

$$H = \frac{I \cdot N \cdot R^2}{2\sqrt{(R^2+x^2)^3}} \quad (6)$$

Where,
N = number of windings of the coil
R = centre of radius *r*
x = distance from the centre of the loop along the x-axis (coil's axis)
At the centre of the loop (*x* = 0), Equation (6) becomes

$$H = \frac{I \cdot N}{2R} \quad (7)$$

For a rectangular loop with edge $a \times b$, the path of *H* can be determined by modifying Equation (6) to give;

$$H = \frac{N \cdot I \cdot ab}{4\pi\sqrt{\left(\frac{a}{2}\right)^2+\left(\frac{b}{2}\right)+x^2}} \cdot \left(\frac{1}{\left(\frac{a}{2}\right)^2+x^2} + \frac{1}{\left(\frac{b}{2}\right)^2+x^2}\right) \quad (8)$$

There is an optimum coil diameter for a reader that ensures that a maximum magnetic field is delivered to the transponder. This diameter can be derived by differentiating *H* with respect to *R*, equating it to zero, and finding the values of R at that point. From Equation (6) [47],

$$H'(R) = \frac{d}{dR}H(R) = \frac{2 \cdot I \cdot N \cdot R}{\sqrt{(R^2+x^2)^3}} - \frac{3 \cdot I \cdot N \cdot R^3}{(R^2+x^2) \cdot \sqrt{(R^2+x^2)^3}} \quad (9)$$

Equating Equation (9) to zero and finding the value of R at that point gives

$$R = \pm x \cdot \sqrt{2} \quad (10)$$

Discarding the negative value (which is just a mirror), the optimum reader coil radius can be described by Equation (10). Although the magnetic force is also a consideration towards establishing the relationship in conductor area. The relationship between the magnetic field intensity *H* and flux density *B* is expressed as

$$B = \mu_0 \cdot \mu_r \cdot H = \mu \cdot H \quad (11)$$

2.4 Power Transfer Theory

Maximum power transfer does not translate to maximum power transfer efficiency [48]. Maximum power is transferred from a source to the load when the load resistance is equal to the equivalent or input source resistance. Taking reference from equation (12), maximum power transfer, at NFC frequency occurs at

$$Q = \frac{2\pi f L}{R} \quad (12)$$

$$R_{ref\,21_3} = \frac{k_{12}^2 Q_1 Q_{2_3}\left(R_s + R_{p1}\right)}{1 + k_{23}^2 Q_{2_3} Q_{3L_3}} \quad \text{(a)} \qquad (13)$$

$$R_{ref\,31_2} = k_{23}^2 Q_1 Q_{3L_2}\left(R_s + R_{p1}\right) \quad \text{(b)}$$

Equation (13) (a) Represents the 3-coil system, while (b) represents the 2-coil system. Q is the quality of the coil, as defined in Eq. (12). R_{pi} is the equivalent resistance of the coil -i; $R_s$is the source resistance of the NFC reader. $k_{ij}$is the coupling coefficient between coil $i$and coil j and $Q_i, Q_L$are intrinsic and loaded values of Q indicated in Eq. 13 (b).

3. METHODOLOGY

The NFC modelling and simulation were done using the Keysight's PATHWAVE Advanced Design System (ADS) Premier High-Frequency and High-Speed Design Platform (2020). It was chosen because of its fast speed high frequency simulation power, and ease of designing. It also has robust simulation engines, a large library of components, and a tuning interface where parameter values can be tuned and observed in real-time. In addition, the design platform also comes with an Application Extension Language (AEL), a C-like functional language that can be used for the expansion of functionalities. Two simulation engines were used to obtain different values used throughout the work – S-Parameters and Transient. The S-parameters simulation was used when the antenna scatter parameters for frequency response and reflection values were required. The Transient simulation was used when time response was required. The Transient Simulation engine is also responsible for generating the high frequency signal used for the simulation. The entire NFC system is modelled into four parts: Reader, NFC Interface, Transponder and NFC Supply, as depicted in Fig. 1.

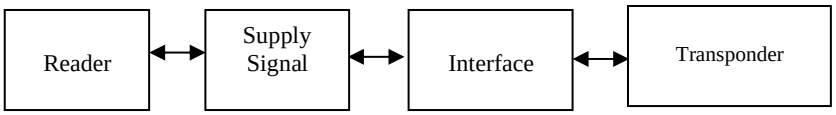

Figure 1. Experimental NFC System model

3.1. The Reader

The NFC Reader is the active component of the NFC system that generates the magnetic field that activates the transponder, and the clock signal with which data is transferred. In this work, a generic NFC reader [10] has been modelled with ADS as a parallel RLC block with a series resistor and a signal source, as shown in Figure 2. The relationship between the power transmitted (which can be determined with the reader current i_r) and the source voltage U_1 as shown in Equation (14) is defined by Ohms law.

$$i_r = \frac{U_1}{Z_c + R_{\text{rel}}} \tag{14}$$

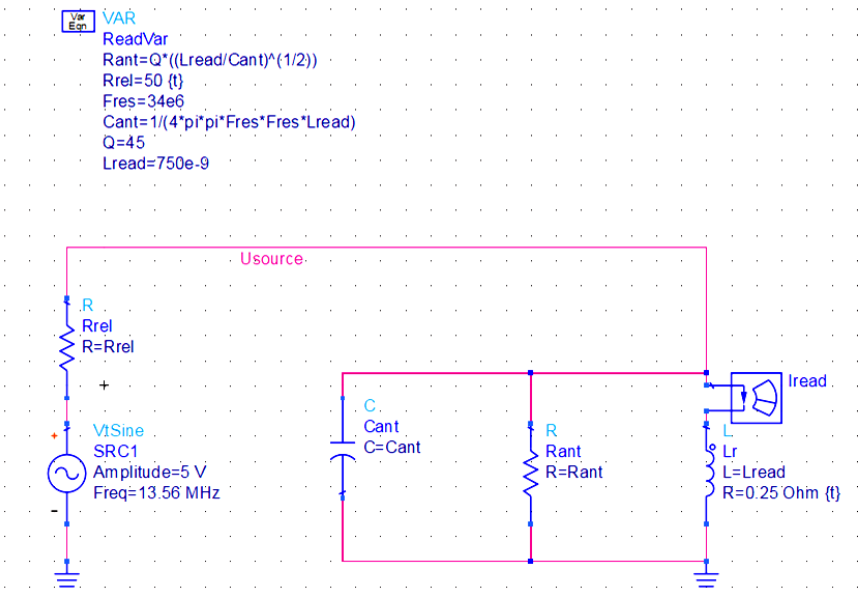

Figure 2. Modelled NFC Reader Module Schematic on ADS

Z_c is the impedance of the reader coil (as described), and can be determined using the simple relation in Equation (17). Equations (15) and (16) describe the relationship between parameters used in the modelling of the reader, as illustrated in Table 2.

$$C_{\text{ant}} = \frac{1}{4\pi^2 \cdot L \cdot f_{\text{res}}^2} \tag{15}$$

$$R_{ant} = Q \cdot \sqrt{\frac{L}{C}} \tag{16}$$

Table 2 Simulation Parameters

Parameter	Symbol Name	Value	
Component		**Reader**	**Tag**
Signal Source	SRC1	5 V, 13.56 MHz	Not applicable
Resistance	R_{rel}	50 Ω (tuneable)	4.2 Ω (tuneable)
Coil Inductance	L_{read}, L_{tag}	750 pH	5.00943 µH
Inductor Series Resistance	R	0.25 Ω	0.85 Ω
Coil Resonance Frequency	F_{res}	34 MHz	13.56 MHz
Coil Q	Q	45	72
Antenna Capacitance	C_{ant}		As in Equation 2.6a
Antenna Resistance	R_{ant}		As in Equation 2.6b
Number of Coils (reader, tag)	n_1, n_2	4	3
Coil Radius	r_1, r_2		3cm, 8cm

Equations **Error! Reference source not found.** and **Error! Reference source not found.** describe the relationship between parameters used in the modelling of the reader, as illustrated in Table.

$$C_{\text{ant}} = \frac{1}{4\pi^2 \cdot L \cdot f_{\text{res}}^2} \quad (16a)$$

$$R_{ant} = Q \cdot \sqrt{\frac{L}{C}} \quad (16b)$$

3.2 The Reader Antenna Matching Network

For maximum power transfer to take place, it is important that the source impedance matches as close as possible to the load impedance. A matching network is a combination of passive network components which are placed in such a way that their impedance effectively matches the load and the source impedances. It was observed that; the reader source is purely resistive $Z_{source} = 50\Omega$ since there are no reactive components, while the load has a reactive impedance that can be determined as in (17).

$$Z_{load} = \frac{1}{\sqrt{\left(\frac{1}{R}\right)^2 + \left(\frac{1}{X_L} - \frac{1}{X_C}\right)^2}} \quad (17)$$

The reflection coefficient before matching is indicated in Figure 3. The marker m1 shows a maximum reflection at 34 MHz and -48.64 dB. The requirement is that the reflection should occur around 13.56 MHz and at maximum power; therefore, the Smith Chart Matching Utility of ADS is employed.

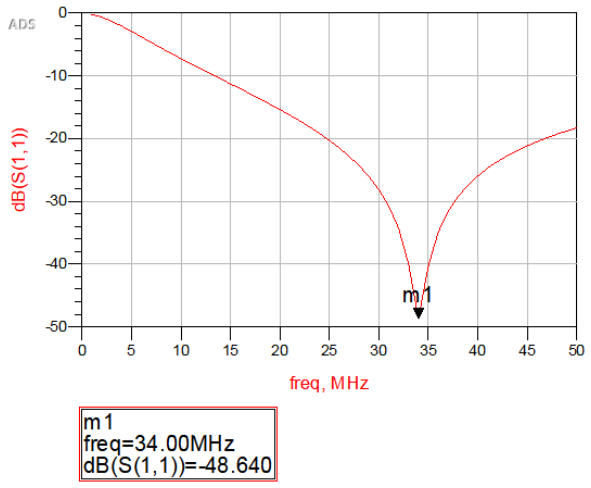

Figure 3. Reflection Coefficients for the Reader Antenna before Matching

A terminator port (TermG) is used for the S-Parameters (Scatter Parameters) simulation to get the reflection coefficient (S_{11}) of the antenna for impedance matching. Fig. 4 is a plot of the reader's antenna reflection coefficient against frequency after introducing the impedance matching network and after matching with Network Response. Figure 4 shows the Smith Chart Utility window and the network response when the impedance is matched.

The Smith Chart component is now added to the schematic model, and the new reflection coefficient is obtained from simulation as seen in Fig. 5. It can be seen from the marker that the coil antenna now has a minimal reflection at 13.56 MHz, as required. For the final schematic used to model the reader. Figure 6 shows

the smith chart matching utility added between the source impedance and the load impedance. It has a negligible effect on the reader coil current.

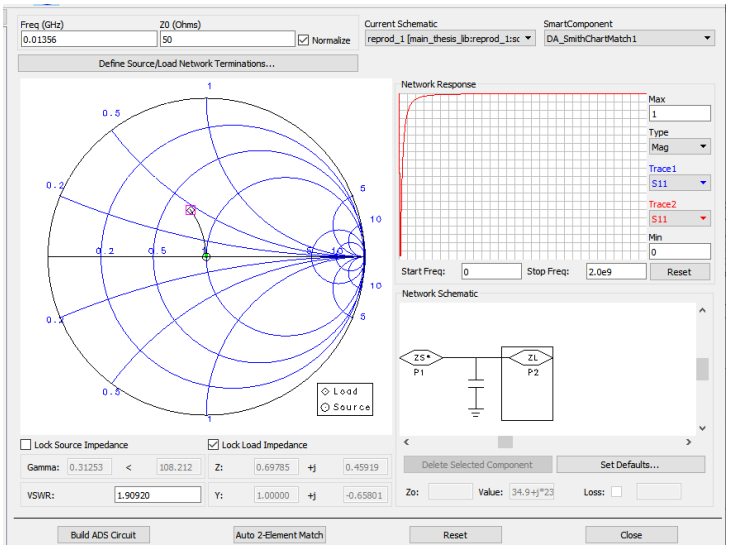

Figure 4. Reflection Coefficients for the Reader Antenna showing response before impedance Matching

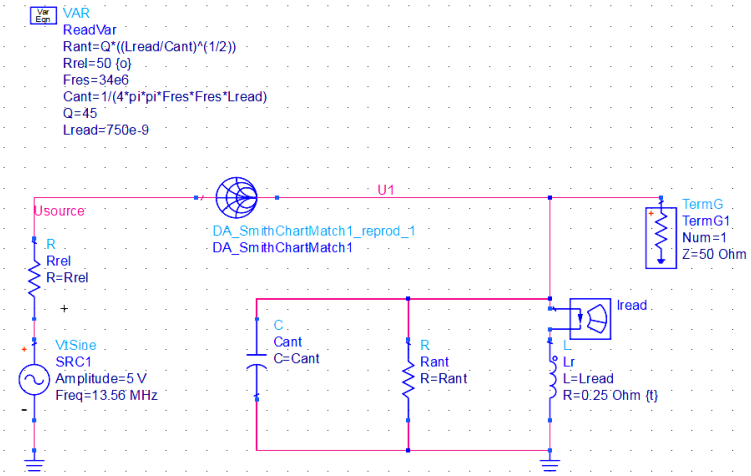

Figure 5. Modelled NFC Reader Module Schematic with Smith Chart Marching Network on ADS

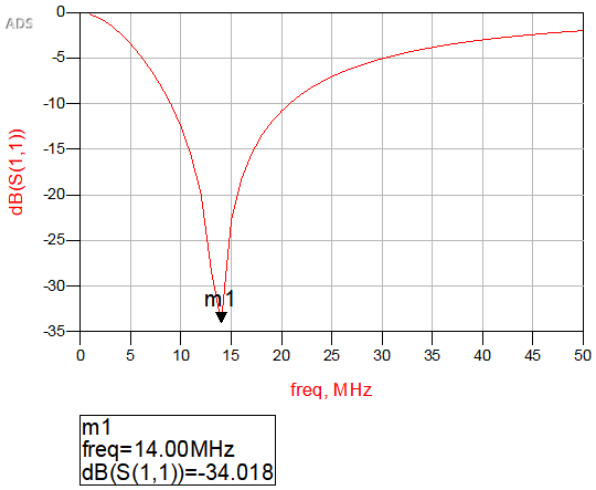

Figure 6. Reader Reflection Coefficient with Matching Network

This NFC interface represents the magnetic field interaction between the reader and transponder. The modelled transponder is the MAX66242 DeepCover Secure Authenticator with ISO 15693, I²C, SHA-256, and 4Kb User EEPROM. It is modelled as a resonance circuit with its coil connected to a series load resistor. Furthermore, the NFC supply is considered in this work as the power transfer function in a physical relation factor. This affects the power transfer between the reader and transponder. The physical relation factors include the distance between the cores, the alignment of the transponder relative to the reader, and the load (which is the operation being undertaken by the transponder). It is assumed that the transponder is perfectly aligned with the reader and that a singular function is always being executed by the transponder, implying that the load is constant. For simulation purposes, the determination of the PTF on ADS is accomplished by using special functions written with Application Extension Language (AEL). These special functions are called during runtime, and are used to determine the PTF at every point during the transaction. This is then used to dynamically scale the magnetic field strength that the reader transmits and, in that way, control the power received by the transponder.

3.3. Optimization Technique

Towards fulfilling the objective of this research, minimization of power dissipated by the reader on the tag is important. Power is controlled by varying the reader coil series resistance. The only two variables under which the power can be controlled are the power transfer function (PTF) and output voltage. Power is transferred by inductive coupling between the reader and the transponder to zminimize the power consumption from the card reader, while preserving the functionality of the entire system. Figure 7, shows the optimization process flow used in this study.

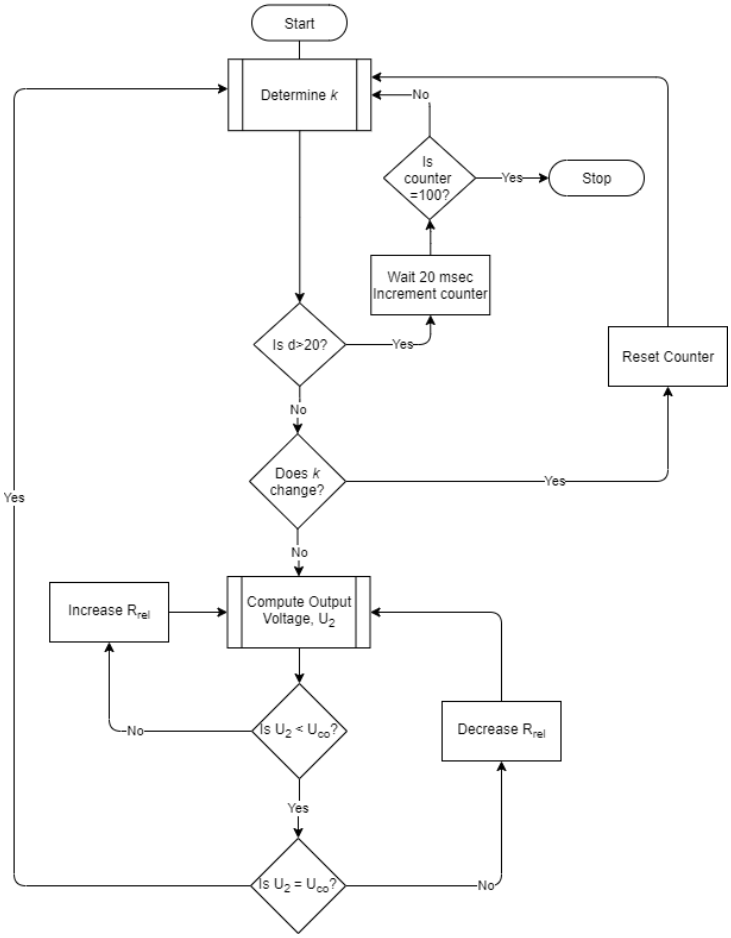

Figure 7. Optimization Process Flow

4. RESULTS AND DISCUSSION

The NFC system was simulated with the Keysight *Advanced Design System*, and the detail of result are presented in this section. The NFC system was simulated with the Keysight *Advanced Design System*, and the detail of the result are presented in this section. The tuning component of the ADS, together with the ability

to sweep through variables, was used to model changes in the physical relation factors. For the purpose of simplicity, the simulation was done over a range of distances between the coils, from 0 cm to 20 cm. Also, to allow tracing a particular value over a range of distances, 5 µsec was used as a benchmark time. The results first capture the I/V Characteristics of the reader-tag system before the optimization. Various current and voltage characteristics values of the reader – tag system was simulated before the optimization. Figures 8a and 8b shows the sinusoidal AC source voltage (5V amplitude) and the reader corresponding current before the optimization. It can be observed that for a time period of 5 µsec, there is no change in both the voltage and current trends. The reader still dissipates the same amount of power, irrespective of the load.

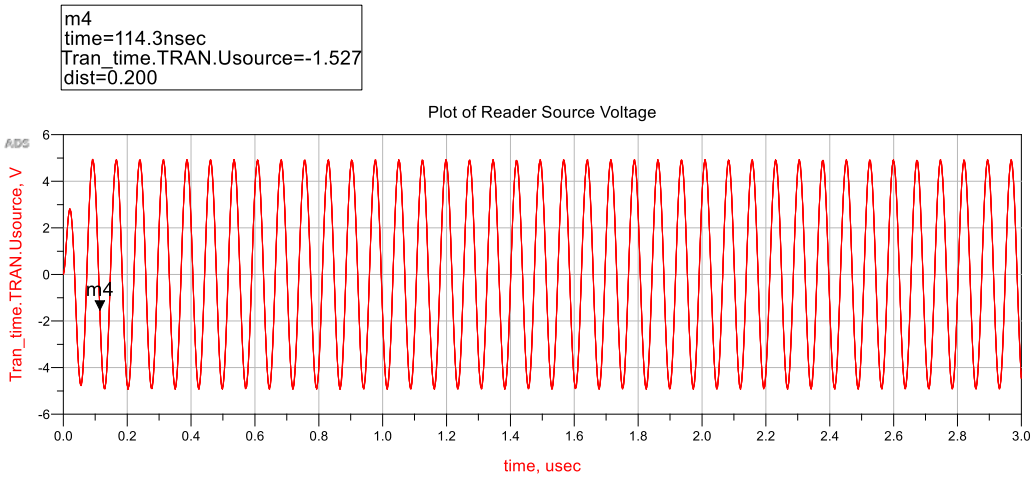

Figure. 8a. Reader Source Voltage before Optimization

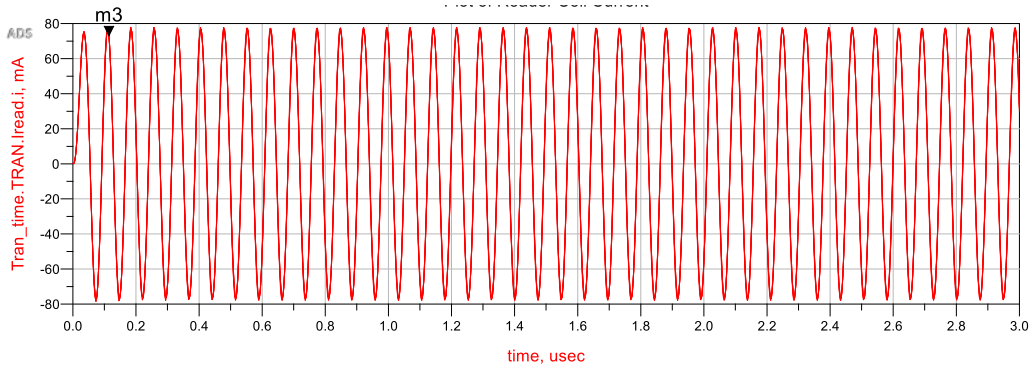

Figure 8b. Reader Source Coil Current before Optimization

The markers tracked the values of both voltage and coil current values when the ADS code was run and implemented (Figure. 9). Considering the induced voltage and rectified voltage; a comparison between the source voltage and induced voltage at different distances was considered. It was observed that the source voltage is independent of the distance, while the induced voltage is not. This induced voltage was analyzed and used for the adaptive H-field scaling.

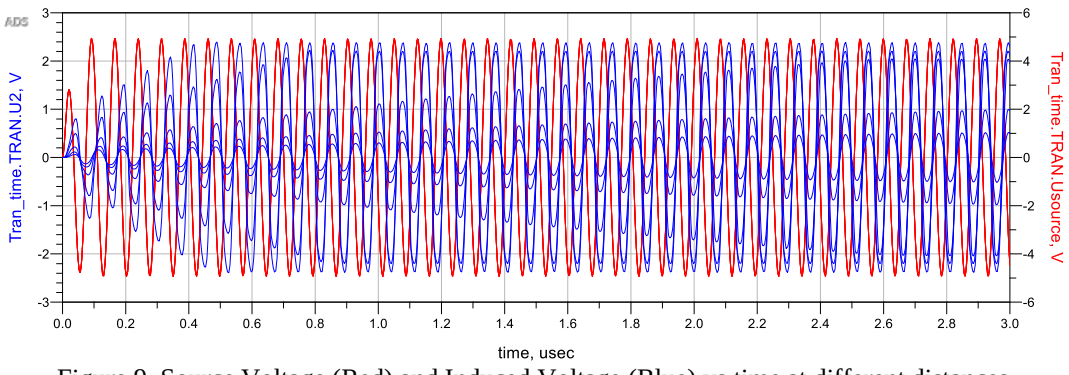

Figure 9. Source Voltage (Red) and Induced Voltage (Blue) vs time at different distances

The composite plot in figure 10 displays the induced and rectified voltage at different distances. It can be seen from the plot that the rectified voltage has no negative component and has a higher peak value of 3.8 V, while the induced voltage is sinusoidal with a peak of 2.4 V. It is also worth observing that the rectified voltage is maximum at a distance of $x = 0$ cmand minimum at $x = 20$ cm.

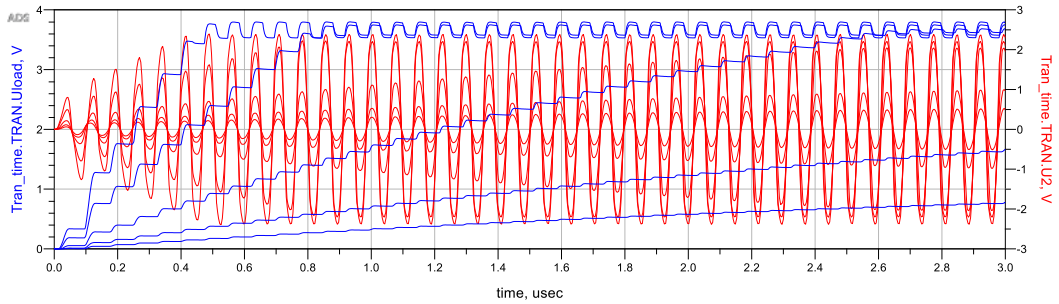

Figure. 10. Induced (blue) and Rectified (red) voltage vs time at different distances

Tag (load) Characteristics, unlike the reader characteristics, the tag (or load) characteristics are entirely dependent on the physical relation factors. With the use of a sweep variable of distance under the constraints of 0 cm to 20 cm in 5 steps, various plots were derived from the product of simulation (Figures11 and 12) with respect to load out voltage distribution across varying distances as well as their corresponding tag current distances. At a d = 0 cm, the load receives maximum current at 0.5 µsec was inferred. Traces of the tag voltage at the particular time stamp of 5 µsec was observed. Simulation shows a steady drop until 10 cm when the tag becomes undersupplied.

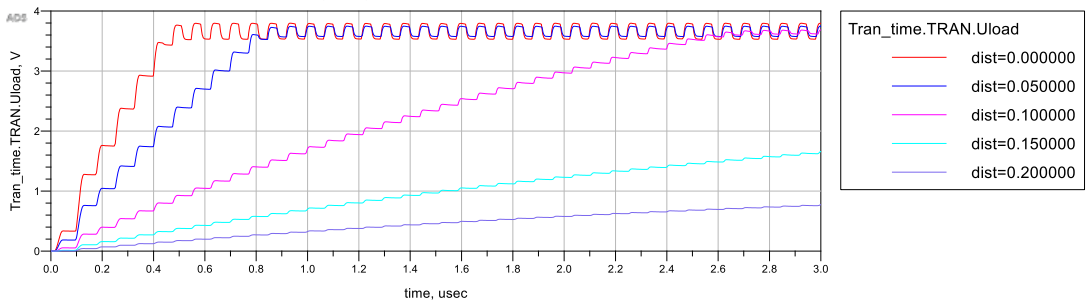

Figure 11. Load Output voltage at different distances

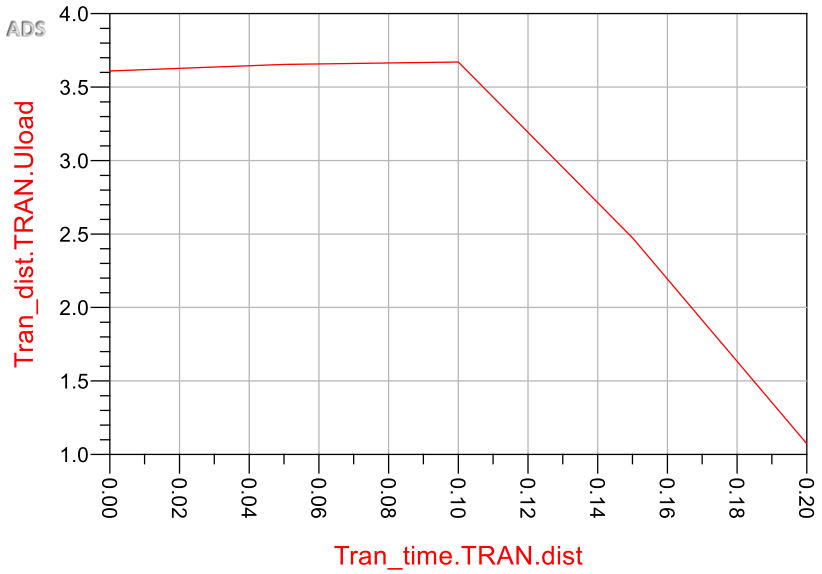

Figiure 12. Load voltage distribution and distance at 5 µsec

Similarly, in Figure 13; the power delivered to the load is minimum at $d = 20$ cm, because the coupling is minimum.

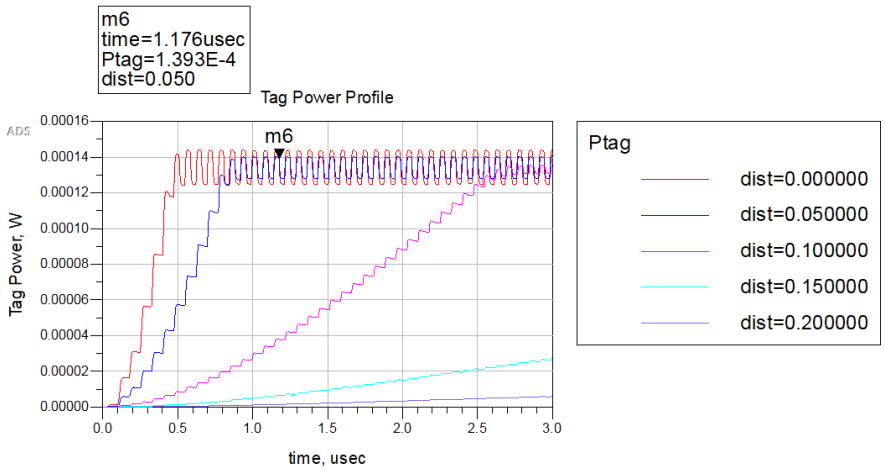

Figure 13. Tag Power usage at different distances

Similarly, the result of the coupling coefficient k characteristics simulation using d = 0 cm, and d = 20cm are presented in Figures 14 and 15. In addition, it is also evident that the magnitude of the load voltage is dependent on the value of *k*. Instantaneous values of *k* are plotted against load voltage at different distances (Fig. 16). The power dissipated by the reader is determined by multiplying the source voltage and coil current.

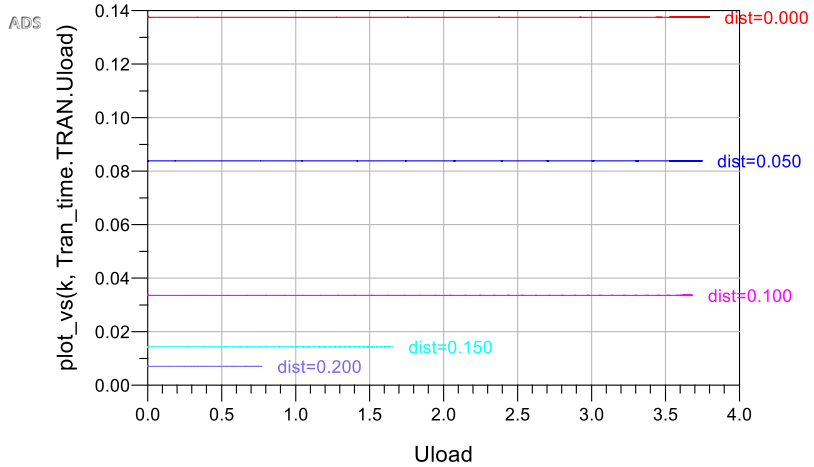

Figure 14. Comparing the values of *k* against load voltage at different distances

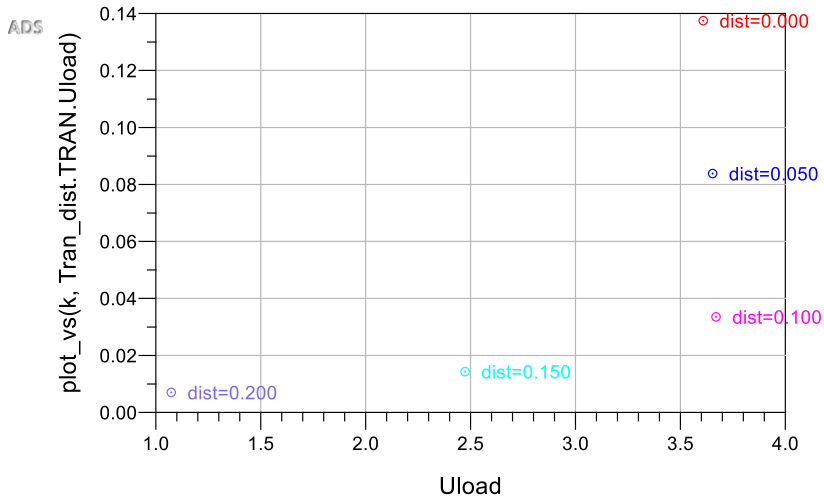

Figure 15. Instantaneous *k* values vs Load voltage at 5 µsec in different distances

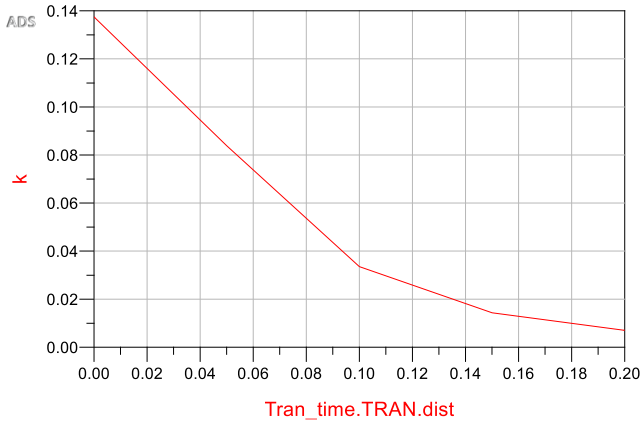

Figure 16. Variation of k values at 5 µsec

Table 3 shows the values of the power dissipated by the reader (obtained by calculation) from the simulated values at 500 µsec over 5 distance values. Figure 17 shows a plot of the power dissipated by the reader before the optimization algorithm is applied, based on Equation 4.1.

$$P_{\text{read}} = i_r \cdot U_1 \quad (4.1)$$

Table 3. Reader Power Values before optimization at 500 µsec over 5 distance values.

Time (µsec)	Pread				
	dist=0.000	dist=0.050	dist=0.100	dist= 0.150	dist=0.200
500.0 µsec	0.008	0.004	0.001	0.002	0.003

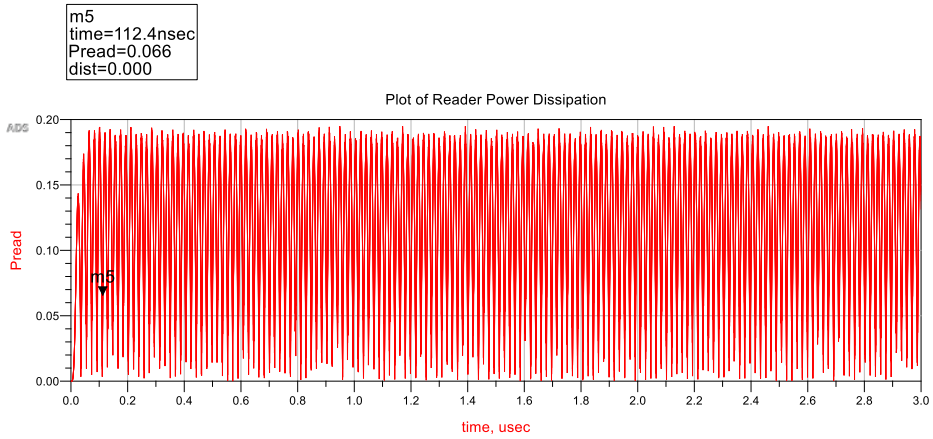

Figure 17. Power dissipated by the reader before optimization

Following a successful optimization algorithm application, some changes were observed from power dissipation and *H*-field as shown in Figure 18 - a plot that displays the power dissipation by the reader. The source voltage witnessed little or no change by the optimization, as described earlier.

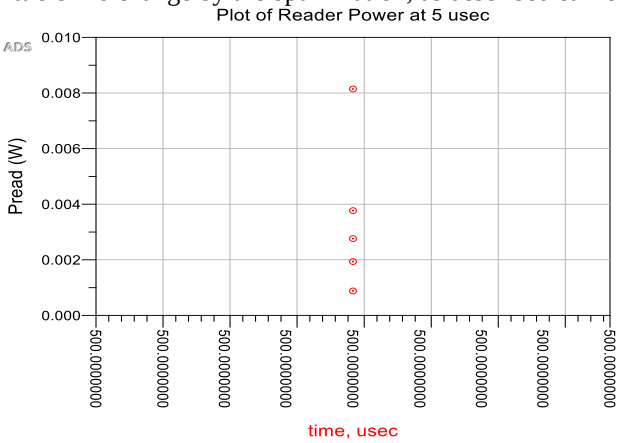

Figure 18. Instantaneous Power Dissipated by the reader

Simulations of the most notable metric (*H*-Field), which is the magnetic field around the coils before and after applying the optimization algorithm are indicated in Figure 19 while Table 4 highlights the values of *H* obtained by simulation.

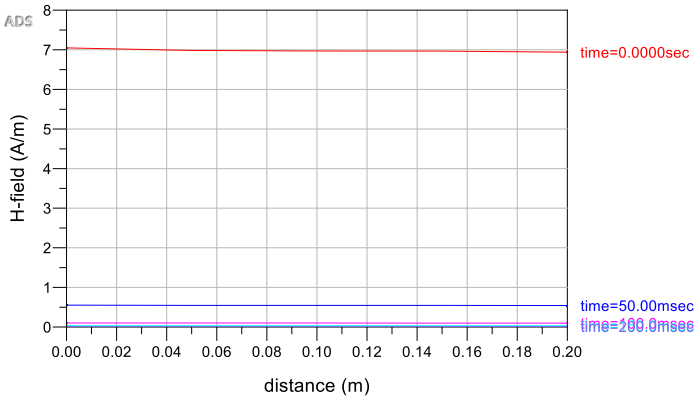

Figure 19. Plot of H-field against distance

Table 4. The distribution of the *H*-field with distance and time

dist (m)	H_field				
	dist=0.000	dist=0.050	dist=0.100	dist=0.150	dist=0.200
0.000	7.045	0.551	0.100	0.033	0.014
0.050	6.984	0.547	0.100	0.032	0.014
0.100	6.969	0.546	0.099	0.032	0.014
0.150	6.965	0.545	0.099	0.032	0.014
0.200	6.940	0.543	0.099	0.032	0.014

The response to change in the physical relation factor (*k*) is only affected by the resistor R_{rel} which acts to alter the coil current are indicated in Figures 20-21.

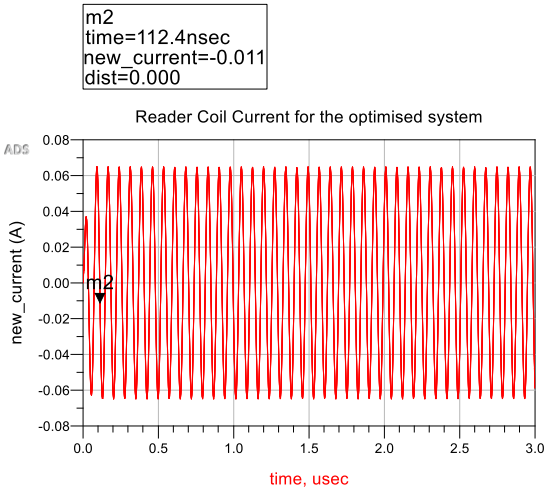

Figure 20. Reader coil Current for the zoptimized system

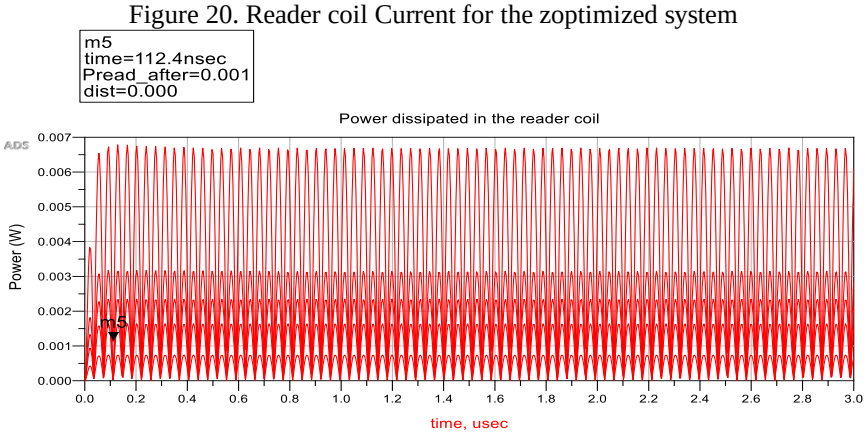

Figure 21. Optimized Reader coil Current and Reader Power Dissipation

Using the same marker, it can be observed from figure. 21 that the power dissipated in the coil in the unoptimized system is 66 times the power dissipated in the zoptimized system given the same conditions. This represents a 98% decrease in power usage. The H-field of the optimized system is responsive to change in distance, are presented in Table 5 and figure 22.

Table 5. H-field of 5 distances for the zoptimized system

Dist (m)	H_Field_new
0.000	0.182
0.050	0.017
0.100	0.016
0.150	0.009
0.200	0.008

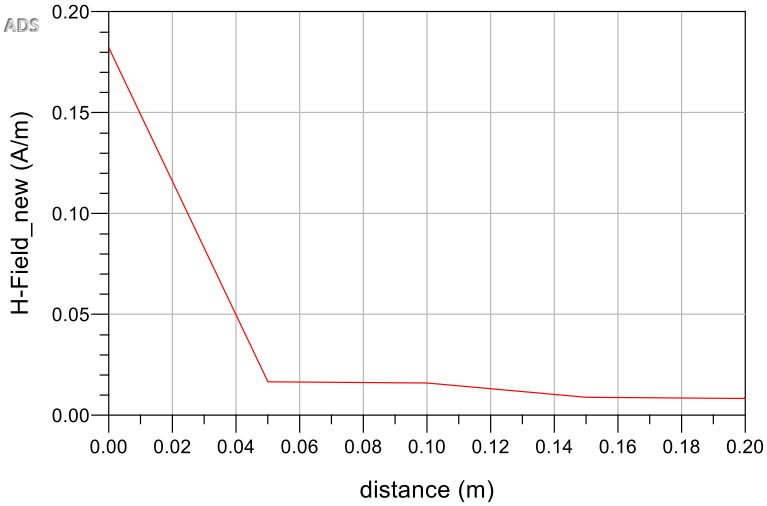

Figure 22. Plot of the H-field for the zoptimized system

5. CONCLUSION

In this study, an improved communication algorithm was developed. The outcome is an algorithm that minimizes the loss of energy in NFC systems by using dynamic field strength scaling. The proposed algorithm used the ADS design tool for dynamic adjustment of reader coil response based on varying distance of the transponder. The tag action was limited to being read by the reader. The simulation carried out revealed that; given the same conditions, power dissipated by the reader can be reduced by a factor of 66 when the new communication algorithm is employed. The novelty of this study lies in the newly developed algorithm which can subsequently serve as a theoretical reference for future work. The work further tested with a simulation of a typical physical system to guide designers in developing systems using up to five sweeps of distance that employs the strategies described. In future, more sweeps for the simulation and multiple coil geometries will be explored for additional conditions to capture additional parameters such as Packet Error Rate (PER) and Bit Error Rate (BER).

ACKNOWLEDGMENTS

We want to acknowledge the University of Lagos and University of Namibia for providing an enabling environment for this research.

REFERENCES

[1] NFC Forum, "NFC Forum – ISO / IEC 14443 Analog Parameter Comparison and Alignment," no. 1.5, pp. 1–148, 2017.
[2] N. H. Motlagh, "Near Field Communication (NFC) - A technical Overview," University of Vaasa, 2012. doi: 10.13140/RG.2.1.1232.0720.
[3] M. Akafan, B. Minaei-Bidgoli, and A. Bagheri, "Determining the Membership Percentage of Each Node in Overlapping Communities Using Multi-agent Collective Intelligence.," *Eng. Lett.*, vol. 28, no. 4, 2020.
[4] L. Lin, M. Zhang, and L. Ma, "Solving the Telecommunication Network Problem using Vague Graph.," *Eng. Lett.*, vol. 28, no. 4, 2020.
[5] D. Paret, *Design Constraints for NFC Devices*, 1st ed. London: ISTE Ltd, John Wiley & Sons, Inc, 2016.
[6] S. Seneviratne *et al.*, "A Survey of Wearable Devices and Challenges," *IEEE Commun. Surv. Tutorials*, vol. 19, no. 4, pp. 2573–2620, 2017, doi: 10.1109/COMST.2017.2731979.

[7] Adebisi J.A, B. O. Moses, and others, "The Role of Network Technologies in the Enhancement of the Health, Education, and Energy Sectors," *Netw. Commun. Technol.*, vol. 7, no. 1, pp. 1–39, 2022.
[8] Y. Zhao, B. Mahoney, and J. R. Smith, "Analysis of a Near Field Communication wireless power system," *2016 IEEE Wirel. Power Transf. Conf. WPTC 2016*, no. May, 2016, doi: 10.1109/WPT.2016.7498827.
[9] N. Druml *et al.*, "Adaptive field strength scaling - A power optimization technique for contactless reader / smart card systems," *Proc. - 15th Euromicro Conf. Digit. Syst. Des. DSD 2012*, no. October 2015, pp. 616–623, 2012, doi: 10.1109/DSD.2012.20.
[10] M. Menghin, "Power Optimization Techniques for Near Field Communication Systems," Technischen Universität Graz Betreuer, 2014.
[11] D. Cheng, Z. Wang, and Q. Zhou, "Analysis of distance of RFID systems working under 13.56MHz," in *2008 International Conference on Wireless Communications, Networking and Mobile Computing, WiCOM 2008*, Oct. 2008, pp. 1–3. doi: 10.1109/WiCom.2008.703.
[12] M. Menghin, N. Druml, C. Steger, R. Weiss, R. Bock, and J. Raid, "NFC-DynFS: A way to realize dynamic field strength scaling during communication," in *2013 5th International Workshop on Near Field Communication, NFC 2013*, 2013. doi: 10.1109/NFC.2013.6482438.
[13] Y. Zhao, J. R. Smith, and A. Sample, "NFC-WISP: A sensing and computationally enhanced near-field RFID platform," *2015 IEEE Int. Conf. RFID, RFID 2015*, pp. 174–181, 2015, doi: 10.1109/RFID.2015.7113089.
[14] J. Adebisi and D. ALABI, "Design and Implementation of a Predictive Model for Nigeria Local Football League.," *Int. J. Comput. Sci. Secur.*, vol. 15, no. 4, pp. 106–123, 2021.
[15] M. Y. Malik, "Power Consumption Analysis of a Modern Smartphone," *arXiv.org*, Dec. 2012.
[16] H. Lang, "Optimization of Wireless Power Transfer Systems with Multiple Transmitters and Receivers," 2018.
[17] G. Van Damme and K. Wouters, "Practical Experiences with NFC Security on mobile Phones," *RFID Sec*, p. 13, 2009, doi: 10.1145/358438.349303.
[18] S. C. Alliance, "About the Smart Card Alliance," no. August, 2014.
[19] L. Benini, A. Bogliolo, and G. De Micheli, "A survey of design techniques for system-level dynamic power management," *IEEE Trans. Very Large Scale Integr. Syst.*, vol. 8, no. 3, pp. 299–316, 2000, doi: 10.1109/92.845896.
[20] Y. Zhao, H. Li, S. Naderiparizi, A. Parks, and J. R. Smith, "Low-cost wireless power efficiency optimization of the NFC tag through switchable receiver antenna," *Wirel. Power Transf.*, vol. 5, no. 2, pp. 87–96, 2018, doi: 10.1017/wpt.2018.1.
[21] H. Xie, Y. Wu, R. Li, D. Liu, W. Zhang, and Z. Jia, "An Energy-Optimization Method for Multipath Wireless Sensor Networks.," *Eng. Lett.*, vol. 30, no. 1, 2022.
[22] J. Satansup, T. Pukkalanun, and W. Tangsrirat, "High-Input-Impedance Four-Input Single-Output Voltage-Mode Biquadratic Filter with Only VDTAs and Grounded Capacitors," *Eng. Lett.*, vol. 30, no. 2, 2022.
[23] X. Wei, Z. Wang, and H. Dai, "A critical review of wireless power transfer via strongly coupled magnetic resonances," *Energies*, vol. 7, no. 7, pp. 4316–4341, 2014, doi: 10.3390/en7074316.
[24] S. Nikoletseas, T. Raptis, A. Souroulagkas, and D. Tsolovos, "Wireless Power Transfer Protocols in Sensor Networks: Experiments and Simulations," *J. Sens. Actuator Networks*, vol. 6, no. 2, p. 4, 2017, doi: 10.3390/jsan6020004.
[25] X. LIGUANG, S. Yi, H. Y. Thomas, and L. Wenjing, "WIRELESS POWER TRANSFER AND APPLICATIONS TO SENSOR NETWORKS," *IEEE Wirel. Commun.*, no. August, pp. 140–145, 2013.
[26] R. Shadid, S. Noghanian, and A. Nejadpak, "A literature survey of wireless power transfer," in *IEEE International Conference on Electro Information Technology*, 2016, vol. 2016-Augus, pp. 782–787. doi: 10.1109/EIT.2016.7535339.
[27] R. Shadid and S. Noghanian, "A Literature Survey on Wireless Power Transfer for Biomedical Devices," *Int. J. Antennas Propag.*, vol. 2018, pp. 1–11, 2018, doi: 10.1155/2018/4382841.
[28] D. K. Biswas, M. Sinclair, J. Hyde, and I. Mahbub, "An NFC (near-field communication) based wireless power transfer system design with miniaturized receiver coil for optogenetic implants," in *Proceedings of the 2018 Texas Symposium on Wireless and Microwave Circuits and Systems, WMCS 2018*, 2018, pp. 1–5. doi: 10.1109/WMCaS.2018.8400620.
[29] R. Wang, X. Zhou, J. Zheng, and D. Yang, "Research on the Efficiency of Wireless Power Transfer System Based on Multi-Auxiliary Transmitting Coils," in *2017 4th International Conference on Information Science and Control Engineering (ICISCE)*, 2017, pp. 1677–1681. doi: 10.1109/ICISCE.2017.350.
[30] V. Coskun, B. Ozdenizci, and K. Ok, "A survey on near field communication (NFC) technology," *Wireless Personal Communications*, vol. 71, no. 3. pp. 2259–2294, 2013. doi: 10.1007/s11277-012-0935-5.
[31] F. Kneibl, R. Röttger, U. Sandner, J. M. Leimeister, and H. Krcmar, "All-I-Touch as combination of NFC and lifestyle," in *Proceedings - 2009 1st International Workshop on Near Field Communication, NFC 2009*, 2009. doi: 10.1109/NFC.2009.19.
[32] T. Page, "Technological Diffusion of Near Field Communication (NFC)," *Int. J. Technol. Diffus.*, vol. 7, no. 3, pp. 59–75, 2016, doi: 10.4018/ijtd.2016070105.
[33] V. Coskun, B. Ozdenizci, and K. Ok, "The survey on near field communication," *Sensors (Switzerland)*, vol. 15, no. 6, pp. 13348–13405, Jun. 2015, doi: 10.3390/s150613348.
[34] J. Fischer, "NFC in cell phones: The new paradigm for an interactive world [Near-Field Communications]," *IEEE Commun. Mag.*, vol. 47, no. 6, pp. 22–28, Jun. 2009, doi: 10.1109/MCOM.2009.5116794.
[35] J. A. Adebisi and K. A. Abdusalam, "Design and Construction of a Secured Wireless EVoting System Using Crystal Oscillator," in *14th International Conference of the Nigeria Computer Society*, 2019, pp. 194–203.

[36] A. Adebisi J, B. Damilola E, and B. Olubayo M, "A multicriteria framework for selecting information communication technology alternatives for climate change adaptation," *Cogent Eng.*, vol. 9, no. 1, p. 2119537, 2022.
[37] J. A. Adebisi and O. M. Babatunde, "Selection of Wireless Communication Technologies for Embedded Devices using Multi-Criteria Approach and Expert Opinion," *Niger. J. Technol. Dev.*, vol. 19, no. 4, pp. 373–381, 2022.
[38] M. K. Yusof, A. Abel, M. Y. Saman, and M. N. Abdul Rahman, "Adoption of near field communication in S-Library application for information science," *New Libr. World*, vol. 116, no. 11–12, pp. 728–747, 2015, doi: 10.1108/NLW-02-2015-0014.
[39] R. Steffen, J. Preißinger, A. Müller, I. Schnabel, and T. Schöllermann, "Near Field Communication (NFC) in an automotive environment: Use cases, architecture and realization," in *Proceedings - 2nd International Workshop on Near Field Communication, NFC 2010*, 2010, no. 01, pp. 15–20. doi: 10.1109/NFC.2010.11.
[40] J. Merkus, "Security evaluation of the NFC contactless payment protocol using Model Based testing," Open University of the Netherlands, 2018.
[41] M. Badra and R. B. Badra, "A Lightweight Security Protocol for NFC-based Mobile Payments," in *Procedia Computer Science*, 2016, vol. 83, no. Ant, pp. 705–711. doi: 10.1016/j.procs.2016.04.156.
[42] D. Silva-Pedroza, R. Marin-Calero, and G. Ramirez-Gonzalez, "NFC Evaluation in the development of mobile applications for MICE in Tourism," *Sustain.*, vol. 9, no. 11, 2017, doi: 10.3390/su9111937.
[43] R. Tesoriero and J. A. Gallud, "Software architecture and framework to develop NFC-based applications," *Sensors (Switzerland)*, vol. 18, no. 8, 2018, doi: 10.3390/s18082654.
[44] R. Iqbal, D. Saeed, A. Gilani, and H. H. R. Sherazi, "Design of Near Field Communication Passive Antenna for Circular Shaped Wearable Items," no. October, 2014.
[45] B. Lee, B. Kim, and S. Yang, "Enhanced Loop Structure of NFC Antenna for Mobile Handset Applications," *Int. J. Antennas Propag.*, vol. 2014, pp. 1–6, 2014, doi: 10.1155/2014/187029.
[46] M. Menghin, N. Druml, C. Steger, R. Weiss, H. Bock, and J. Haid, "The PTF-determinator: A run-time method used to save energy in NFC-systems," in *Proceedings - 2012 4th International EURASIP Workshop on RFID Technology, RFID 2012*, 2012, no. 1, pp. 92–98. doi: 10.1109/RFID.2012.12.
[47] K. Finkenzeller, *RFID Handbook*, 3rd ed. Munich, Germany: John Wiley & Sons, Ltd. Registered, 2010. doi: 10.1002/9780470665121.
[48] M. N. Abdallah, T. K. Sarkar, and M. Salazar-Palma, "Maximum power transfer versus efficiency," *2016 IEEE Antennas Propag. Soc. Int. Symp. APSURSI 2016 - Proc.*, pp. 183–184, 2016, doi: 10.1109/APS.2016.7695800.

BIOGRAPHY OF AUTHORS

Khadeejah Adebisi Abdulsalam (PhD) Dr. Abdulsalam is a Computer Engineer with interest in communication, computation and energy modeling. She had her undergraduate degree in Computer Engineering and MSc degree in Computer Sciences from Obafemi Awolowo University and a PhD in Electrical and Electronics Engineering from University of Lagos. The PhD thesis is in the area of Computation and Energy Modelling. She is currently teaching Undergraduate and Post graduate courses in University of Lagos. She was the Deputy Director in charge of Network Infrastructure and Services at the University of Lagos, center for Information and Technology Systems from August 2018 to July 2022. Dr Abdulsalam, together with her research team, won a research Grants from the CODESRIA in 2017 which has been completed and has an ongoing Grant with Nigerian Communications Commission for a research work on Rural Broadband Penetration. Dr Abdulsa lam has over 20 publications, she is a COREN registered Engineer.

IJIKE KINGSLEY CHIDOZIE is An Electrical Engineer with Msc in Electrical and Electronics Engineering specialized in communication. Android and Java Developer. IT Specialist. Avid Learner, Founder at ICTech Solutions.

John Addebisi A is a *Senior member of IEEE,* with over 15 International Certifications bagged his undergraduate degree in Computer Engineering, M. Sc degree in computer with specialty in Data Analytics and Business Intelligence and Ph.D. in Software Engineering. He has over 10 years of experience as a software and infrastructure engineer with successful deployments of several Projects across various industries including Banking, Telecommunication, Government and Educational Institutions. He has conducted research in Enterprise Systems Integration, databases and BI/Analytics using Microsoft BI Stack, IOT, Smart Systems, SharePoint-Workflows among others. He mentored many in the industry and Academics with scholarly articles published in top-rated journals. He is Registered Professional Engineer, a Chattered IT Professional and member association of computing machinery, United States.